Quartz-Based Photonic Crystal Surfaces for Multiplexed Cancer Biomarker Detection

C.-S. Huang, V. Chaudhery, J. Polans, M. Lu,
B. T. Cunningham*
Department of Electrical and Computer Engineering
University of Illinois at Urbana-Champaign
Urbana, USA
bcunning@illinois.edu

A. Pokhriyal
Department of Physics
S. George
Department of Bioengineering
University of Illinois at Urbana-Champaign
Urbana, USA

R. C. Zangar
Pacific Northwest National Laboratory
Richland, USA

***Abstract*—We report for the first time the combination of a quartz-based photonic crystal (PC) with a detection instrument designed to perform label-free (LF) and enhanced fluorescence (EF) imaging for antibody microarray applications. Label-free detection is used to quantify binding density of immobilized capture antibodies. Angle-scanning approach is implemented to achieve more uniform fluorescence enhancement by reducing the coefficient of variation of replicate assays by 20-99% compared to ordinary fluorescence microscopy.**

I. INTRODUCTION

Among the techniques for the detection of disease biomarkers, antibody microarrays have proven to be a powerful platform due to their capability for multiplexed detection, minimal reagent usage, and high sensitivity. Sandwich assays are used to increase the sensitivity and specificity of antibody microarrays through the use of a primary antibody to initially capture the analyte from serum, and a second primary antibody that is fluorophore-tagged that recognizes a separate epitope on the same analyte [1]. Recently, the optical resonances of photonic crystal (PC) surfaces have been demonstrated to provide substantial fluorescence excitation enhancement in addition to a 5-10x magnification of the emitted photon collection efficiency for surface-based fluorescent assays such as DNA microarrays and protein microarrays [2, 3]. The PC is comprised of a periodically modulated sub-wavelength surface structure fabricated from a low refractive index material coated with a high refractive index dielectric layer. For PC-enhanced fluorescence (PCEF), the surface is designed to perform as an optical resonator at the wavelengths of fluorescence excitation and fluorescence emission [4]. In addition to providing fluorescence enhancement, detection of shifts in the resonant coupling conditions caused by attachment of biomolecules also allows a PC to serve as a platform for label-free (LF) detection [5]. A high resolution imaging system has been developed for PC surfaces to measure the density of DNA microarray capture spots as a means for quality control [5]. In this work, we demonstrate the combination of a quartz-based PC with a detection instrument designed to perform LF and EF imaging using collimated laser illumination. The EF/LF microscope is used to detect the output of a sandwich ELISA protein microarray with twenty-one breast cancer biomarker assays.

II. METHODS

A. Quartz Photonic Crystal

The fabrication of PC was based on "step-and-flash" nanoimprint lithography (NIL) and detailed previously [6]. This device as shown in Fig. 1a, b was designed to have two resonances at TM-polarization (electric field perpendicular to the grating structure) to support the EF and LF detection modalities through use of two laser illumination wavelengths. The resonance condition of the quartz PC can be observed by measuring the dip in the transmission spectrum when the PC is subjected to broadband illumination as shown in Fig. 1c, where two transmission spectra are shown. When illuminated at normal incidence, the transmission dip is observed at ~690 nm with a full width half maximum (FWHM) of $\Delta\lambda$=3 nm. When light is incident at an angle of 11°, there is a resonance at λ~633 nm with a FWHM of $\Delta\lambda$=4 nm. For the EF detection modality, the PC is designed specifically for Cyanine-5 (Cy5) due to its strong quantum yield and high absorption efficiency at the λ=633 nm wavelength of HeNe lasers. The PC can be tuned to an on-resonance condition by illuminating its surface using a TM–polarized wavelength of λ=633 nm and corresponding incident angle of 11°. This illumination condition will result in an amplified near field electric field intensity on the PC surface for enhanced excitation.

978-1-4577-1767-3/12/$26.00 ©2012 IEEE

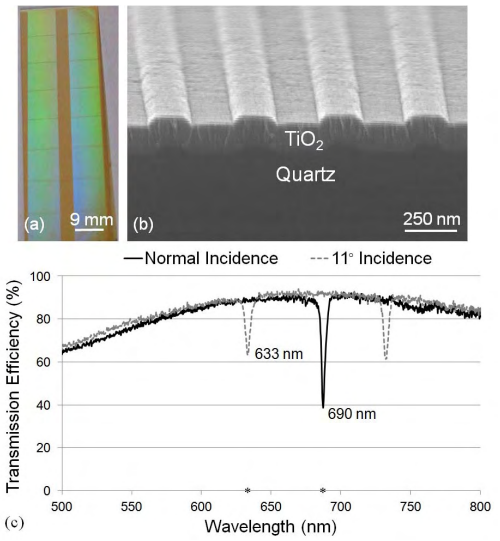

Figure 1: (a) Photograph of a 1 x 3 in^2 PC slide with an 8x2 pattern of 8.75 x 8.75 mm^2 imprinted grating regions, (b) SEM image showing cross section of a PC and (c) transmission spectrum of both normal and 11° incidence. The resonance at λ=690 nm is used for label-free measurement and enhanced extraction of Cy5 emission. The excitation wavelength of λ=633 nm is used for enhance excitation of Cy5.

The large illumination angle is designed to prevent excitation light from coupling into the objective lens and subsequently reaching the detection system. The PC exhibits a second resonance at λ=690 nm, which spectrally overlaps with the emission spectra of Cy5. This resonance is used to more efficiently direct emitted photons towards the detector to obtain enhanced extraction [7]. The resonance at λ=690 nm at normal incidence angle is also used for the LF detection modality where the deposition of capture antibodies on the PC leads to a localized increase in the effective refractive index of the PC resulting in a shift in the resonance angle.

B. Microarray Preparation and Assay Protocol

The microarray preparation and sandwich assay format has been described in detail previously [3]. In brief, a self-assembled monolayer of 3-glycidoxypropyl-trimethoxysilane (GPTS) was applied by a vapor-phase technique. Four replicate spots per assay of capture antibodies were printed in each array on a quartz PC slide using a noncontact printer. Following the printing, the slide was incubated overnight at room temperature and 60% humidity. The slide was then blocked to prevent nonspecific binding and followed by incubating with a mixture of antigens with gentle agitation overnight. The slide was then incubated with a mixture of biotinylated detection antibodies with mild agitation and then followed by incubation with Strepavidin-conjugated Cy5. Finally, the slides were washed and dried before fluorescence and LF measurements.

C. Fluorescence and Label-Free Measurement

In order to measure both LF and EF intensities, the integrated EF/LF microscope system shown in Fig. 2 was used. A detailed construction and description of the instrument has been presented previously [8]. For a fixed incident wavelength of λ=633 nm, the PC resonant coupling condition has a full width half maximum in angle ($FWHM_\theta$) $\Delta\theta \sim 0.4^\circ$. While a narrow resonant coupling condition has been shown to provide the greatest fluorescence excitation enhancement factor, the stringent conditions for optimal laser-PC coupling means that a small deviation of $\Delta\theta=0.4^\circ$ from the true device resonant angle would result in a 50% reduction in fluorescence intensity [9]. Variations in the optimal PC resonant coupling angle across an array can originate from the nonuniformity of the device during the fabrication process, nonuniformity in the surface chemistry layer, and nonuniformity in the density of antibody capture spots – both between spots and within a spot. In order to retain high signal amplification while achieving uniform signal enhancement across the whole microarray slide, an angle-scanning method that accounts for variations in the resonant angle across the slide was developed [9]. Rather than gathering a single fluorescence image using only one incident angle, a sequence of fluorescence images are captured over a range of angles that includes the resonant angle. Image processing software compares the set of images taken at each angle, and selects the maximum intensity for each pixel. The maximum intensity for each pixel corresponds to the incident angle that matches the optimal resonant coupling condition. A composite fluorescence image is generated in which each pixel holds the maximum observed intensity value.

Before immobilizing capture antibodies, the PC resonance is designed to occur at λ=690 nm (when illuminated at normal incidence), resulting in a minimum transmission as shown in Fig. 1c. To obtain LF measurements of the printed antibodies, the λ=690 nm laser was used to illuminate the PC resonance over a range of incident angles near normal incidence. The angle of minimum transmission (AMT) is determined by software on a pixel-by-pixel basis, where shifts in the AMT correspond to locations on the PC with greater immobilized antibody density. Using this technique, a high resolution spatial map of adsorbed captured antibody densities was generated as a function of position on the PC surface.

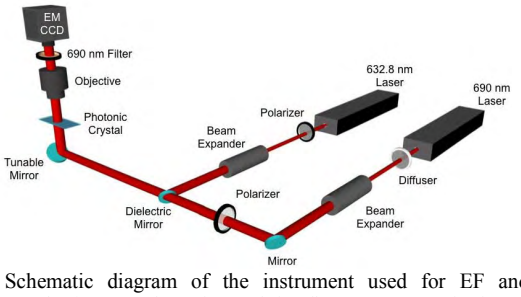

Figure 2: Schematic diagram of the instrument used for EF and LF measurement. The λ=632.8 laser is used for fluorescence excitation, while the λ=690 nm laser is used for label-free imaging. The system incorporates a computer-controlled tunable mirror that is capable of scanning the incident angle through a range of angles. A 4x objective images a 2x2 mm^2 field of view of the PC. The CCD measures transmitted laser intensity as a function of incident angle at λ=690 nm for LF detection, and measures fluorescence emission intensity from the PC for EF detection.

III. Results and Discussion

A. Label-Free Measurement

The LF imaging modality of the detection instrument can be used to characterize the antibody capture spot density on the PC surface. As shown in Fig. 1c, the PC exhibits a resonant reflection at λ=690 nm near normal incidence before the deposition of capture biomolecules. The dielectric permittivity of immobilized biomolecules results in an increase in the resonant coupling angle that is proportional to the adsorbed mass area density, and the coupling angle increase is spatially localized to the regions of the PC surface where the biomolecule attachment occurs. Using computer control, the angle scanning mirror of the detection instrument (Fig. 2) can be rapidly scanned through a range of angles in small increments ($0^\circ < \theta < 3^\circ$ with $\Delta\theta = 0.01^\circ$), and an image of the transmitted intensity can be gathered at each incident angle using the CCD imager. For each pixel, the AMT is determined by mathematically finding the minimum of the plot of transmitted intensity as a function of θ, to generate a spatial map of AMT versus position on the PC surface with pixel resolution of 16 μm. To account for any nonuniformity as described in previous section, two AMT images are gathered. An initial AMT image of the PC surface is obtained prior to deposition of antibody capture spots, and a second AMT is gathered after spot deposition. The two images are aligned and mathematically subtracted (after spots – before spots) to produce a spatial map of the AMT shift due to the deposited capture antibodies. An AMT shift image of one set of immobilized capture antibody spots is shown in Fig. 3a using the layout shown in Fig. 3b. The average net AMT shift of four replicates for each antibody is plotted in Fig. 3c, which depicts the variability of binding density obtained from the antibodies used in our array, despite the use of identical antibody concentrations, buffers, spotting conditions, and incubation conditions. After the deposition of antibodies, the AMT shifts roughly from 0.1° (for EGF and HGF) to 1° (for uPAR). This wide range of resonant coupling conditions suggests that, during the subsequent enhanced fluorescent imaging, using a fixed incident angle to illuminate the entire array could not be expected to provide uniform fluorescence enhancement for every assay. In this work, the LF imaging of microarray capture spots was mainly used to quantify the resonance angle shifts caused by the printed antibody capture spots. The LF detection modality can also be used to identify the presence of missing capture spots, spots with nonuniform antibody density, or other spatial features that would render a capture spot useless for further analysis [5].

B. Angle-Scanning to Achieve Uniform Enhancement

As discussed previously, the PC enhanced excitation effect is highly sensitive to the resonant angle for collimated illumination. For the PC used here, $FWHM_\theta < 0.4^\circ$. Therefore, a small deviation in illumination angle from the actual resonant angle results in a significant drop in the signal enhancement. As indicated in the LF measurement, upon deposition of antibodies, the resonance angle can shift from $0.1^\circ < \Delta\theta < 1^\circ$, depending on the density of the capture antibodies, thus it is necessary to adjust the incident angle of fluorescent illumination to achieve the maximum enhancement for each spot. Rather than using a single fixed angle to scan the entire array, a series of 300 fluorescent images were captured for incident angle range of $10.5^\circ < \theta < 12.5^\circ$ at increment of $\Delta\theta = 0.01^\circ$. The 4× objective used in EF/LF microscopy system yields a 2x2 mm^2 field of view which covers one of the replicates shown in Fig. 4a. For the angle-scanning method, it takes 9 seconds to capture 300 images to generate a final composite image for one replicate.

The maximum intensity values for each pixel are used to generate a composite fluorescent image in which each pixel is represented at its optimal on-resonance coupling condition. For comparison, a single fixed angle intentionally selected at an off-resonance condition ($\theta = 12.2^\circ$) for an array is shown in Fig. 4a, while the angle-scanning approach was used to generate the fluorescence image shown in Fig. 4b. GenePix Pro 6.1 software was used to quantify the median spot intensity. The CV were calculated as the standard deviation divided by the average of these median spot intensities of four replicate spots for each assay. The CV for each detection approach is compared in Fig. 4c, in which the angle-scanning method improves the CV by up to 99%. We observe that assays with the greatest antibody capture spot density, as measured by the AMT shift image, do not correlate to higher fluorescence intensities for detection of biomarkers. We also observe that variability in the capture spot density does not correlate strongly with the CV of fluorescence signals (correlation coefficient ~0.5). Due to variability in capture molecule/analyte affinity and capture molecule activity, we do not observe a strong correlation between the fluorescent signal and the LF signal, therefore we do not apply a correction factor to the fluorescent measurement that compensates for capture antibody variability, so that, higher antibody density does not necessarily result in greater sensitivity for detection of the corresponding biomarker.

IV. Conclusion

In this work, we demonstrate a novel optically active PC surface and detection method that can substantially augment protein microarray analysis in two distinct ways. A quartz PC fabricated by nanoimprint lithography was demonstrated as a surface that can simultaneously support enhanced fluorescence and label-free measurement using a custom-made detection instrument. The device structure is designed to produce two distinct and narrow resonant modes that enable two complementary imaging modalities to be performed in the same detection instrument. The LF detection modality is used to quantify and visualize binding density variability of immobilized capture antibodies as a means for providing quality control and spot-quality screening. We introduced an angle-scanning fluorescence imaging approach for PCEF that automatically corrects for variability in optimal resonant coupling conditions that originates from the observed variability in antibody capture spot density. The ability of the angle-scanning method to provide high uniform fluorescent enhancement throughout an array was demonstrated through a substantial reduction in fluorescent intensity CV, as compared to measuring the same array with off-resonance illumination at a single angle.

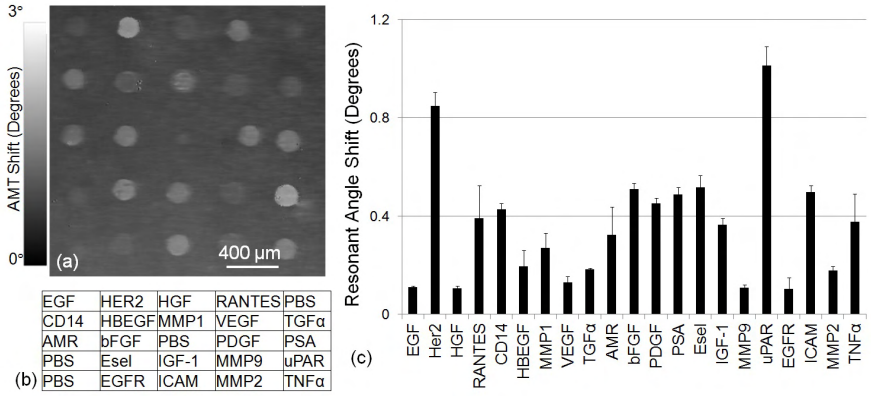

EGF	HER2	HGF	RANTES	PBS
CD14	HBEGF	MMP1	VEGF	TGFα
AMR	bFGF	PBS	PDGF	PSA
PBS	Esel	IGF-1	MMP9	uPAR
PBS	EGFR	ICAM	MMP2	TNFα

EGF Her2 HGF RANTES CD14 HBEGF MMP1 VEGF TGFα AMR bFGF PDGF PSA Esel IGF-1 MMP9 uPAR EGFR ICAM MMP2 TNFα

Figure 3: Label-free characterization of the density of antibody capture spots by measuring shifts in the □=690 nm resonance. (a) Image of the shift in the Angle of Minimum Transmission (AMT) for a representative array of antibody capture spots, representing a label-free measurement of the capture spot density. (b) Layout of the capture antibodies within an array. (c) Average net AMT shift values for the capture antibodies with error bars representing one standard deviation of from four replicate arrays on the same chip. Measurements indicate a large variability in capture spot density that is dependent on the specific antibody, but excellent reproducibility for a particular antibody. AMR, amphiregulin; bFGF, basic fibroblast growth factor; CD14, cluster of differentiation 14; EGF, epidermal growth factor; EGFR, epidermal growth factor receptor; Esel, E-selectin; HBRGF, heparin-binding epidermal growth factor; Her2, c-erbB-2 extracellular domain; HGF, hepatocyte growth factor; ICAM, intracellular adhesion molecule 1; IGF-1, insulin-like growth factor 1; MMP1, matrix metalloprotease 1; MMP2, matrix metalloprotease 2; MMP9, matrix metalloprotease 9; PDGF, platelet-derived growth factor AA; PSA, prostate specific antigen; RANTES, regulated on activation normal T cell expressed and secreted; TGFα, transforming growth factor alpha; TNFα, tumor necrosis factor alpha; uPAR, urokinase-type plasminogen activator receptor; VEGF, vascular endothelial growth factor.

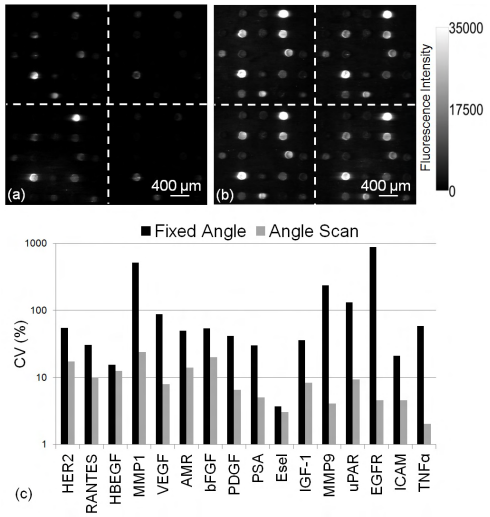

Figure 4: (a) Fluorescence images from both (a) fixed angle method and (b) angle-scanning method from the third highest concentration. (c) Bar chart of CV comparison between two scanning methods shows that angle-scanning method greatly improves the uniformity of spot intensities.

The combination of a quartz PC with a custom detection instrument that can optimally couple laser illumination into multiple PC resonances can be used as a platform for a wide variety of surface-based fluorescence assays that would benefit from reduction of detection limits and the ability to measure the density of capture molecules.

ACKNOWLEDGMENT

This work was supported by the National Institutes of Health (Grant No. GM086382A), and the National Science Foundation (Grant No. CBET 07-54122). Any opinions, findings, conclusions, or recommendations expressed in this material are those of the authors and do not necessarily reflect the views of the National Institutes of Health or the National Science Foundation.

REFERENCES

[1] R. M. Gonzalez, S. L. Seurynck-Servoss, S. A. Crowley *et al.*, "Development and validation of sandwich ELISA microarrays with minimal assay interference," *Journal of Proteome Research,* vol. 7, no. 6, pp. 2406-2414, Jun, 2008.

[2] P. C. Mathias, S. I. Jones, H. Y. Wu *et al.*, "Improved Sensitivity of DNA Microarrays Using Photonic Crystal Enhanced Fluorescence," *Analytical Chemistry,* vol. 82, no. 16, pp. 6854-6861, Aug, 2010.

[3] C. S. Huang, S. George, M. Lu *et al.*, "Application of Photonic Crystal Enhanced Fluorescence to Cancer Biomarker Microarrays," *Analytical Chemistry,* vol. 83, no. 4, pp. 1425-1430, Feb, 2011.

[4] N. Ganesh, W. Zhang, P. C. Mathias *et al.*, "Enhanced fluorescence emission from quantum dots on a photonic crystal surface," *Nature Nanotechnology,* vol. 2, no. 8, pp. 515-520, Aug, 2007.

[5] S. George, I. D. Block, S. I. Jones *et al.*, "Label-Free Prehybridization DNA Microarray Imaging Using Photonic Crystals for Quantitative Spot Quality Analysis," *Analytical Chemistry,* vol. 82, no. 20, pp. 8551-8557, Oct, 2010.

[6] A. Pokhriyal, M. Lu, V. Chaudhery *et al.*, "Photonic crystal enhanced fluorescence using a quartz substrate to reduce limits of detection," *Optics Express,* vol. 18, no. 24, pp. 24793-24808, Nov, 2010.

[7] F. Yang, and B. T. Cunningham, "Enhanced quantum dot optical down-conversion using asymmetric 2D photonic crystals," *Optics Express,* vol. 19, no. 5, pp. 3908-3918, Feb 28, 2011.

[8] I. D. Block, P. C. Mathias, N. Ganesh *et al.*, "A detection instrument for enhanced-fluorescence and label-free imaging on photonic crystal surfaces," *Optics Express,* vol. 17, no. 15, pp. 13222-13235, 2009.

[9] V. Chaudhery, M. Lu, A. Pokhriyal *et al.*, "Angle-Scanning Photonic Crystal Enhanced Fluorescence Microscopy," *Ieee Sensors Journal,* vol. 12, no. 5, pp. 1272-1279, May, 2012.